A HYBRID NUMERICAL-ANALYTICAL APPROACH FOR MODELING LEVITATION BASED VIBRATION ENERGY HARVESTERS

C. Martín Saravia, José M. Ramírez, Claudio D. Gatti

Grupo de Investigación en Multifísica Aplicada, Universidad Tecnológica Nacional FRBB – CONICET – 11 de Abril 461, Bahía Blanca, Argentina.

ABSTRACT

This paper presents a computational approach for the evaluation of the electro-mechanical response of levitation based vibration energy harvesters. A detailed analysis of the relevant physical, mathematical and computational aspects of the design of a harvester is presented. Several key points of the design of levitation based energy harvesters, such as the existence of the resonance phenomenon, the influence of damping in the system response, the magnetic force nonlinearity and the calculation of the magnetic flux derivative for multi-magnet configurations are addressed. The evolution in time of the electromechanical variables is investigated through a hybrid numerical-analytical approach. The evaluation of the levitational force and the magnetic flux derivative is done through a nonlinear model based on the finite element method. A performance assessment is done by comparing the results obtained with the present formulation against measurements; a physical prototype of a multi-pole-multi-coil harvester is built ad hoc. An excellent agreement between the mathematical model and the experiments was found.

1. INTRODUCTION

Vibration energy harvesting is increasingly gaining the attention of the scientific community [1–6]; both the evolution of harvesters and the advances in power consumption of electronic devices is making possible to think of a near future where many electronic devices operate self-energized; however, challenges regarding power density and effective construction still persist.

Levitation based electromagnetic energy harvesters are an interesting alternative for scavenging energy from vibration sources, especially for low frequency applications; the simplicity of its construction together with its low maintenance are points that justify this fact. Investigations about levitation based harvesters are not abundant; a few works can be found in the literature [7–12]. Most of this works are based on an analytical formulation for the magnetic field, which implies that the magnet geometry must be simplified. Several important aspects such as the optimal design of multipole configuration, the accurate modeling of the levitation force, the analysis of the nonlinear response, etc. have still not been addressed.

Zhu and Zu [11] presented the simulation of a vibration-based energy harvester that uses a magneto-electric laminate composite to harvest energy from the nonlinear vibrations of a levitating magnet. A cubic law was used to model the levitation force and an average axial flux analytical formula was used to calculate the axial magnetic flux.

Abed et al. [13] studied the non-linear dynamics of a two degrees of freedom levitation based harvester. The magnetic forces were calculated with simplified analytical expressions; the bandwidth enhancement possibilities of the 2 DOF system was studied. It is not stated in the paper how the magnetic flux was obtained.

Mann and Sims [10] have investigated the design and analysis of a novel energy harvesting device that operates as a tunable oscillator. The researchers proposed a cubic polynomial law for modeling the magnetic force, the coefficients of the polynomial were obtained experimentally. The electromechanical coupling was modeled through a damping coefficient, also obtained experimentally. The response of the system for harmonic excitation was obtained analytically through the method of multiple scales; the dynamics of the system was compared with experiments. No information about the magnetic field distribution and power curves was presented.

Soares dos Santos et al. [8] have reported a levitation based harvester with a single Neodymium moving magnet. The authors developed a semi-analytical approach based on a surface current model for calculating the magnetic flux distribution; the equation of motion were integrated numerically. The force between the magnets was obtained through derivative of their interaction energy; this requires the assumption that the magnets are coaxial. Friction between the magnet and the cylinder was considered through a Karnopp model. Some sort of finite rotation framework in terms of Euler angles was presented to account for container arbitrary dynamics; although, the non-commutativity of rotations was not addressed.

Lee et al. [14] also presented a levitation based harvester composed of a single magnet moving inside a coil. Both cubic and quintic polynomials were used to model the magnetic force between the moving magnet and the end magnets. The coefficients of the polynomial were obtained experimentally. The electromechanical coupling was also obtained through experiments. The magnetic flux was assumed to be uniform and constant in time; thus the variation of the magnetic field with the displacement of the moving magnet was not considered.

Munaz et al. [15] studied different design architectures of an electromagnetic harvester. The magnetic flux density was modeled with analytical functions; the superposition principle was recalled when multipole magnets were studied. A finite element analysis was conducted to find the optimal magnetic flux distribution according to the number of poles of the moving magnet. Experimental analyses were conducted and compared against the power calculated assuming that the magnet moves according a sinusoidal law; so, the dynamic of the system was imposed and the electromechanical coupling was neglected. The coil configuration used to avoid cancellation in the multipole configuration was not informed.

Apo and Priya [9] studied the effect of multipole configurations for the moving magnet of a levitation based harvester. The levitating force equation was found to be a cubic polynomial. Finite element analysis was conducted to find optimal magnet configuration. No details about the solution of the equations of motion were given.

Dallago et al. [16] developed an analytical model for considering the nonlinear stiffness effect on levitation based harvesters. A cubic law for the magnetic force was used; the polynomial coefficients were found through FEM.

Avila Bernal and García [17] presented a mathematical derivation for modeling the dynamics of mono-pole electromagnetic energy harvesters. Analytical models for the magnetic field distribution and magnetic force were presented. The analytical results were compared against FEM.

A different class of levitation based harvesters are diamagnetic levitation harvesters; these devices completely avoid the use of containers and therefore friction is eliminated from the problem. In this direction, Wang et al. [18] and Palagummi et al. [12] have developed a harvester with dual diamagnetic plates and a cylindrical levitating magnet.

Some important conclusions can be made analyzing the cited works; the magnetic flux was modeled with analytical expressions or even not modeled at all. This is a important fact since the correct modeling of the magnetic flux density is crucial to obtain an accurate prediction of the generated power and also of the levitation force. Some works claim the analytical modeling of the magnetic flux is superior to numerical modeling in terms of accuracy and computational cost [8]. Although it could be possible to justify the contrary, it suffices to say that analytical approaches only can deal with very simplified geometries. Note that still the involved formulations used by Santos et. al [8] and Avila Bernal and García [17] to model the axial magnetic flux distribution cannot account for the effect of the flux interference caused by the end magnets nor the effect of spacers in multipole magnets. Accurate analytical modeling of the magnetic flux distribution for levitating harvesters is possible only for simple magnet geometries.

This work presents a general mixed formulation for modeling linear electromagnetic energy harvesters. The work is focused on the development of a computational procedure to predict the time variation of the induced voltage in a complex energy harvester. The approach is based on a hybrid formulation that is capable of dealing the most general case of linear harvester configuration. The evolution of the mechanical variables is obtained through an analytical model while the magnetic variables are obtained through the finite element method. Both models are linked through a series of computational routines that involve: polynomial fitting, numerical integration and data lookup algorithms.

The magnetic flux density is calculated using finite elements; a computational algorithm extracts the average flux as a function of the axial coordinate and calculates its derivative via a central difference scheme. The levitation force at discrete locations is also obtained with the same finite element

data, thus avoiding the use of analytical expressions which are limited to single-pole magnets. This also avoids the use of experimentation to obtain the force law. A polynomial fitting technique is used to finally obtain an analytical force-displacement function.

The equations of motion of the electromechanical system are written as a function of the average flux derivative; then they are transformed to the state space in order to be solved through a numerical integration algorithm.

The approach is capable of modeling devices with arbitrary magnet geometry, arbitrary magnet pole and coil counts, and random mechanical excitations. Several nonlinear affects, such as: frictional, viscous and electromagnetic damping are naturally included in the model. The proposed approach has great flexibility and generality of a full tridimensional coupled electromechanical simulation and still retains the simplicity of one dimensional approaches. The validation of the formulation is done through a detailed comparison against experimental data obtained from physical testing of a prototype multi-pole multi-coil harvester built ad hoc. Also, some key aspects of levitation based harvesters, such as the jump phenomenon and its sensitivity to the system friction and load amplitude are briefly addressed.

2. ELECTROMECHANICAL DESIGN

The reported Levitation Based Vibrational Energy Harvesters (LBVHs) have a similar architecture; a magnet or stack of magnets moves inside a cylinder that is surrounded by a coil. The motion of the magnet is limited by a repulsive force exerted by the opposing magnetic field of auxiliary magnets placed in the cylinder ends. In this work, we propose a multi-coil-multi-magnet-multi-spacer configuration of a LBVEH, see Figure 1. The objective of this design is to generate a complex voltage-time signal and then test the proposed approach in this complex scenario. In order to simplify the language, the central magnet assembly of magnets and spacers will be called "stack".

The design of the harvester starts with the study of the behavior of the dynamical system; this requires to find the equations that describe the force interaction between the components. The repulsive force exerted by the auxiliary end magnets is nonlinear with the distance between them and the moving magnet; thus, they play the role of a nonlinear stiffness. The magnets repulsive force law can be reasonably approximated with a polynomial [9,11,16,19]; since it is the responsible of the stability of the dynamical system, odd power functions are required.

A LBVEH is designed to recover energy from vibration sources, the nature of the source constraints the harvester tuning. There is a common misinterpretation in most research works, the harvester is said to be designed to have a resonant frequency that is coincident with the predominant frequency of the source [9,11,15,16,20]. This is not strictly correct since an LBVEH do not have a resonant frequency; it is known the fact that an oscillator with nonlinear stiffness can be modeled by the Duffing's equation, which do not exhibit resonance [21].
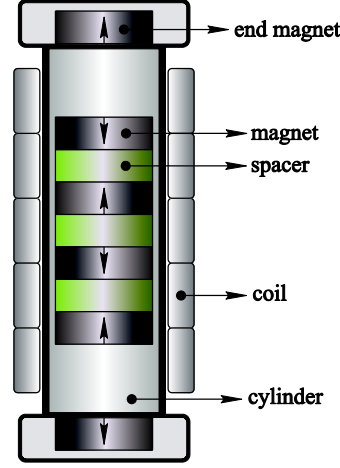
202
203

204 **2.1. Electro-mechanics**

205 The principle of work of a LBVEH is Faraday's law; as the stack of magnets
206 move inside the cylinder, the magnetic flux through the coils changes with time;
207 inducing an electric field in the coil. This electric field generates an electro-
208 motive force $\mathcal{E}$; this is equal to:

$$\mathcal{E} = \oint_C \boldsymbol{E} \cdot d\boldsymbol{l} = -\frac{d}{dt}\int_S \boldsymbol{B} \cdot \boldsymbol{n}\, dA = -\frac{d\varphi}{dt} \tag{1}$$

209 where $\boldsymbol{E}$ is the electric field, $\boldsymbol{B}$ is the magnetic flux density, C is the curve
210 described by the coil, S is the surface enclosed by the coil loops, $\boldsymbol{n}$ is the surface
211 unit normal vector and φ_m is the magnetic flux through S.
212 So, the total voltage induced in a coil loop is obtained through the integral
213 of the electric field over the curve described by the loop; using Faraday's law
214 this results to be equal to the time derivative of the total magnetic flux through
215 the surface enclosed by the loop [22].
216 Since the stack is contained by the cylinder, it can only move in the axial
217 direction x; the loops enclosed surfaces have a unit normal vector that is
218 coincident with the axial direction. Therefore, the problem is uniaxial and the
219 magnetic flux is only a function of the axial coordinate. Then the induced voltage
220 can be written as

$$V = -\frac{d\varphi_m}{dx}\frac{dx}{dt} = -\varphi'\dot{x} \tag{2}$$

221 where the overdot (˙) indicates time derivative and the accent superscript
222 indicates derivative respect to x.
223 The discrete evaluation of the magnetic flux derivative is possible, so

$$V = -\left(\sum_{i=1}^{nc}\int_S B'(x_i)\, dA_i\right)\dot{x} = -\sum_{i=1}^{nc}\varphi_i'\,\dot{x} \tag{3}$$

224 where A_i is the area of the *ith* coil and B_i' is the x derivative of the x component
225 of the magnetic flux density and nc is the total number of coils. The last equation
226 clearly shows that in order to generate maximum voltage both the magnetic flux
227 derivative and velocity of the stack must be optimized.

228   Now, the equations of motion of the mechanical system can be derived from
229 Newton's law, so

$$F(x, \dot{x}, \varphi_m, t) = m\ddot{x}_s \tag{4}$$

230 where F is the sum of all the forces acting on the stack, m is the stack mass and
231 $\ddot{x}_s$ is the stack acceleration. The forces acting on the system are:

$$F = F_k(x, \varphi_m) + F_c(\dot{x}, \varphi'_m) + F_g \tag{5}$$

232 where F_k is the levitation force, F_c is the damping force and F_g is the gravitational
233 force.

2.2. The magnetic force

235   As previously said, the restoring forces acting on the stack are exerted by the
236 end magnets; as the stack moves into the cylinder the end magnets play the role
237 of a spring. The opposing magnetic fields of the end magnets and the stack
238 generates a stabilizing force that is function of the distance between them. The
239 magnitude of the displacement and the geometric design of the device governs
240 the law of the magnetic force; in general, it is strongly nonlinear.
241   The magnitude of the magnetic force can be obtained through different
242 approaches, the most used are the Gilbert Model [21], the Ampere model and
243 Finite Element Analysis. The Ampere and Gilbert models are analytical
244 approaches that require some level of geometric idealization of the magnets and
245 they are not suitable to model multipole configurations.
246   In the present work, Finite Element modeling was used to obtain the force-
247 displacement law of the harvester; the computer code FEMM was used to
248 perform the simulations [23]. Figure 2 shows a typical magnetic field density
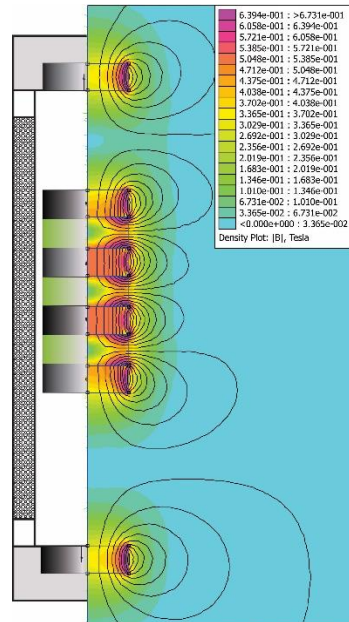249 contour in the device.

250
251 *Figure 2 - Magnetic field density distribution*

252   From the algorithmic point of view, it is strongly desirable to dispose of an
253 analytical function of the magnetic force; this greatly simplifies de evaluation of
254 the both the force vector and the stiffness matrix in the equations of motion.

255   Thus, after calculation the magnetic force for discrete values of the stack
256   position, we used a curve fitting technique to obtain the analytical force
257   displacement function. We found that for the present configuration the magnetic
258   force can be approximated with the following function of the stack displacement

$$F_k = a_0^k u_s + a_3^k u_s^3 + a_5^k u_s^5 \qquad (6)$$

259   where a_i^k are constant parameters and u_s is the displacement of the stack
260   relative to the cylinder base. The Figure 3 shows the magnetic force curve fitting
261   for a given configuration of magnets, cylinder and stack.
262   At this point, it is important to mention that in most works a cubic
263   polynomial is used to represent the magnetic force [9–11,17]. However, in
264   certain cases a cubic polynomial may not be a good choice when the
265   displacements are small since it could lead to instabilities since near the
266   equilibrium point, see Figure 3. This problem can be alleviated if the cubic
267   polynomial fit is done without data gathered when the magnets are closed
268   together (*Cubic Reduced* curve in Figure 3); however, the prediction in for large
269   displacements is greatly deteriorated. A polynomial of fifth order has none of
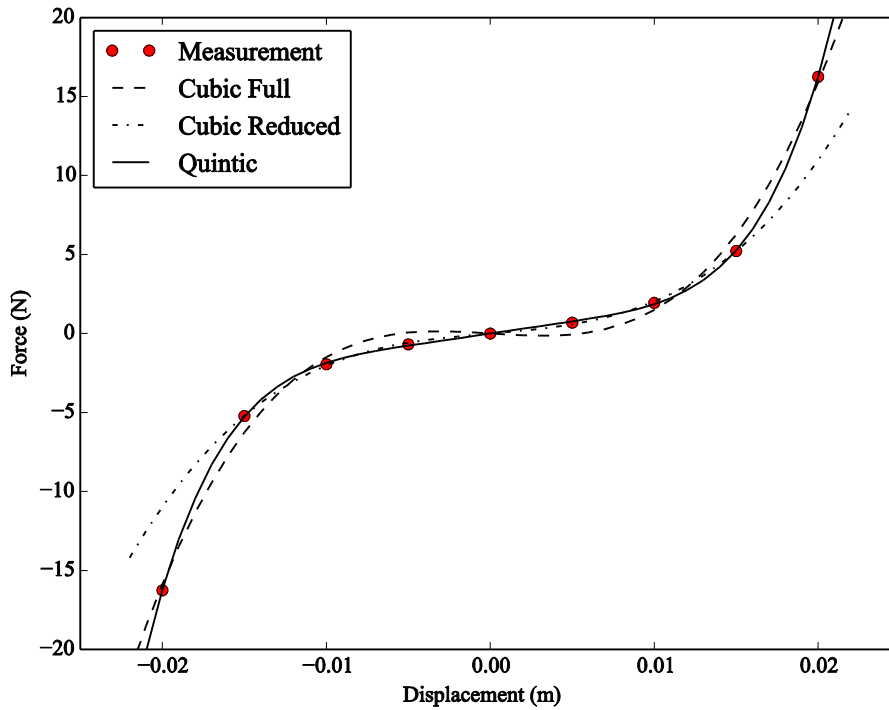270   this inconveniences and thus it is here chosen to represent the magnetic force.

271

272 *Figure 3 - Magnetic force*

273   To obtain a centered function, the initial position of stack was taken at the
274   middle point of the cylinder length; then, the relative displacement of the stack
275   can be written as

$$u_s = x_s - x_b - l_{sb} \qquad (7)$$

276   where x_s is the stack position, x_b is the base position and l_{sb} is the initial
277   magnet-base distance. Note this choice implies that the gravitational load must
278   be imposed to the model.

2.3. The damping force

Damping forces have sometimes been included in the study of the dynamics of LBVEH. Although, its impact on the amplitude of the response is commonly remarked, its influence on the frequency response has certainly not been analyzed. Also, the damping coefficients have been considered independent of the response. As it will be shown later, not only the damping forces are strongly dependent on the harvester response but the response itself is determined to a great extent, both in frequency and amplitude, by the damping.

There are three main sources of damping in a LBVEH: friction, air damping and electromagnetic damping. Air and electromagnetic damping are proportional the velocity, while friction damping is near constant with velocity.

The relative velocity of the stack can be obtained by derivation of Eq. (7) as

$$\dot{u}_s = \dot{x}_s - \dot{x}_b \tag{8}$$

The air damping is the result of the air flux through discharge holes made in the harvester to avoid internal air compression. The simplest, but yet effective, model that can be written to account for air damping is a proportional viscous model; therefore, the air damping force will be obtained as:

$$F_c^s = c_s \dot{u}_s, \tag{9}$$

where is the viscous damping coefficient that will be obtained by identification.

The frictional force can be obtained using a Coulomb model as

$$F_c^f = c_f sign(\dot{u}_s) = \frac{c_f}{|\dot{u}_s|} \dot{u}_s. \tag{10}$$

To derive a unique damping coefficient, it is convenient to rewrite the above equation as

$$F_c^f = \frac{c_f}{|\dot{u}_s|} \dot{u}_s. \tag{11}$$

The induction damping force is generated when the circuit is closed with a load, and thus a current is created. This current creates its own magnetic field; this new magnetic field opposes to its cause, giving rise to a force that opposes the motion. Since this force is proportional to the current and thus proportional to the relative velocity of the stack, it is often considered as an electromagnetic damping force. So, it can be written as

$$F_c^m = c_m \dot{u}_s, \tag{12}$$

where c_m is the electromagnetic damping coefficient.

To derive the expression of the electromagnetic damping an energy balance law must be recalled. The electromagnetic damping force is responsible for the electric power generation, so the energy conversion must be such that the mechanical power dissipated by the electromagnetic damping is equal to the generated electrical power, i.e.

$$F_c^m \dot{u}_s = \frac{V^2}{R_l + R_c + j\omega L_c}, \tag{13}$$

where V is the induced voltage, R_l is the load resistance, R_c is the coil resistance, L_c is the coil inductance and F_c^m is the electromagnetic damping force.

Using Eqs. (3) and (12), the above equations give the electromagnetic damping coefficient as

$$c_m = \frac{(\sum \varphi_i')^2}{R_l + R_c + j\omega L_c} \tag{14}$$

315   At low frequencies the coil inductance has a negligible effect compared to
316   that of the resistance, so the above equation can be written as:

$$c_m = \frac{(\sum \varphi_i')^2}{R_T}, \tag{15}$$

317   where R_T is the total resistance of the circuit.
318
319   NOTE 1: It must be mentioned that it is not possible to mitigate the effects
320   of the electromagnetic damping using repelling pole configurations, as
321   incorrectly stated in [9]. From Eqs. (3) and (15) it is possible to see that in order
322   to reduce the electromagnetic damping, the total flux derivative should decrease,
323   and then the generated voltage is also reduced.

324   **2.4. Inductive performance**

325   As Eq. (2) shows, the maximization of the induced voltage implies the
326   maximization of the product of the velocity and the magnetic flux derivative. So,
327   the efficiency of an electromagnetic harvester is governed by two factors: its
328   dynamics and its induction capability.
329   The induction capability is dependent on the magnetic field gradient strength
330   of the moving magnet, the number of coil loops count and loops area. An
331   analytical law is commonly used to model the magnetic flux distribution along
332   the axial and radial components [8,10,11,14,17]. Sometimes this law is used for
333   multi-magnet stacks, assuming additivity, without proving its validity.
334   The magnetic field gradient strength can be optimized for certain
335   configurations of the stack by using ferromagnetic spacers; the geometrical
336   design of both spacers and the magnets are of key importance to ensure a high
337   flux derivative. The effect of ferromagnetic spacers on the magnetic flux
338   derivative is remarkable, unfortunately it cannot be modeled by analytical
339   approaches. The spacers allow the flux spatial derivative to grow and also
340   change sign; it can be said that they work as backirons. The growth is such that
341   if one replaces the spacers by magnets the flux derivative is considerably lower.
342   The Figure 4 shows a comparison of the flux derivative for a four magnet stack
343   and three spacers configuration vs. a seven magnet stack configuration.

344

345   *Figure 4 - Magnetic flux derivative, effect of spacers*
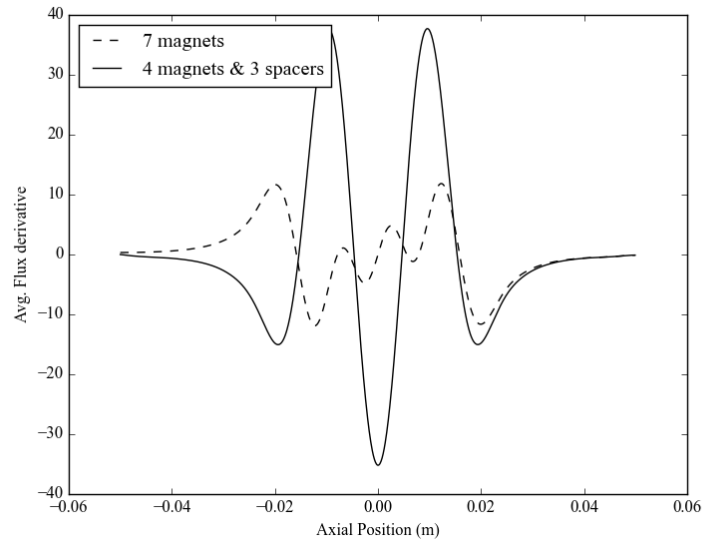
346   The accurate evaluation of the magnetic field distribution is of paramount
347 importance for the prediction of the harvester performance. The Finite Element
348 Method is probably the best tool for that purpose; it is simple, fast and it can
349 handle arbitrary geometries. Claims that the solution of a magnetic finite
350 element problem is time consuming are not true; for example, the evaluation of
351 the magnetic flux distribution generated by a stack of 6 magnets and 3 spacers
352 is solved in less than a second. Neither, modeling time should not be a concern;
353 the generation of the FEM model of the mentioned architecture has taken the
354 authors 5 minutes using FEMM [23]. Also, the construction of a typical LBVEH
355 finite element model could be done by pure coding, thus allowing both
356 parametric and optimization studies.

357   In order calculate the flux derivative at a certain location and time instant
358 we propose an algorithmic approach that processes the magnetic finite element
359 information and operates numerically on the result to obtain a vector of flux
360 derivatives. This vector in conjunction with a 1-D interpolation algorithm to
361 evaluate the flux derivative in every coil of the harvester in a certain time instant.

362   The algorithm has the following procedural structure:

363   I.   Read the finite element results of the magnetic flux (Lua Script).
364   II.   Calculate the average flux density over the coil area in the origin of
365   the axial coordinate (Lua Script).
366   III.   Store the coordinate and the average flux in an ASCII file (Lua Script).
367   IV.   Advance a step in the coordinate and repeat I-III until the last
368   coordinate length (Lua Scritp).
369   V.   Read the average flux file (Python).
370   VI.   Derivate the average flux vector using central difference (Python).
371   VII.   Smooth the derivative using a Savitzky-Golay filter (Python).

372   There is an important point that must be considered for calculating the
373 magnetic flux of a LBVEH; the end magnets perturb the flux in the stack. This
374 perturbation may be not important if the stack is not moving significatively, but
375 can be of importance if the stack moves close to the end magnets. This raises
376 an important problem, since now the magnetic flux distribution is changing with
377 the magnet displacement, and then with time. The Figure 5 shows how the
378 magnetic flux derivate changes its shape as the stack moves closer to the end
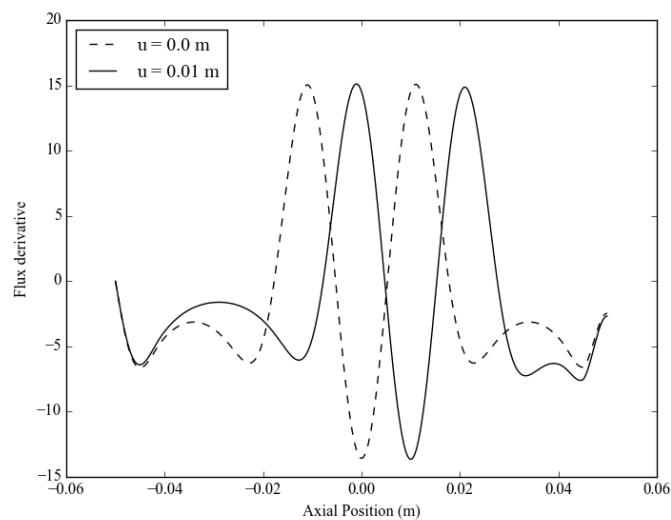379 magnet.

380

381   *Figure 5 - Magnetic flux derivative*

382   The last assertion can also be confirmed analyzing the magnetic flux contour
383   from Figure 6.
384

385
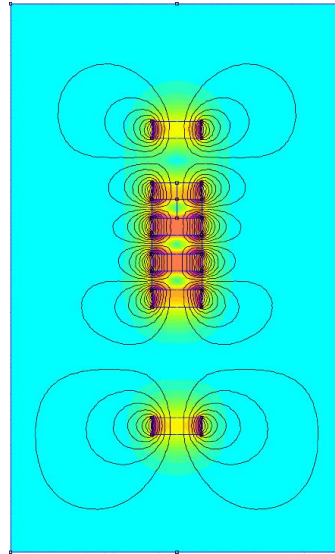386   *Figure 6 - Magnetic flux derivative*

387   The variation of the magnetic flux pattern with the magnet displacement
388   pose a question about the necessity of considering this variation in the
389   determination of the generated voltage. From the computational point of view,
390   considering the flux variation is cumbersome; two approaches could be used to
391   tackle the problem: a full finite element analysis of the coupled problem or a so-
392   called quasi-static determination of the flux for different locations of the magnet
393   with a subsequent point searching technique to determine the flux after the
394   solution of the dynamic problem. Fortunately, the change in the flux derivative
395   is accompanied with a reduction in velocity of the stack; which implies that, still
396   when the magnetic flux distribution is perturbed by the magnets close up, the
397   effect on the voltage generation may not be important. For the sake of brevity,
398   this effects will be disregarded in the present paper; although, it will be treated
399   in a future work.
400   It is important to note that a multi-coil configuration requires an out of phase
401   connection of the coils; otherwise the group of coils would behave as a large
402   single coil and thus the term multi-coil would be incorrect.

403   **2.5. Power optimization**

404   The optimization of the harvester power generation capability implies the
405   maximization of the integral of the product of the velocity and the magnetic flux
406   derivative. The source vibration imposes the operating conditions of the
407   harvester; therefore, its optimal design requires knowing the time and frequency
408   characteristics of the source signal.
409   The most simplified model of a LBVEH could be well represented by the
410   Duffing's equation; the dynamics of the Duffing's equation is well known, and it
411   could be well justified that, unlike linear systems, vibration amplitudes raise
412   unlimitedly with frequency.
413   It is commonly accepted that an effective harvester should be tuned to work
414   in a resonant condition [9,10,12,13,15,16,20]. However, magnetic harvesters do
415   not   exhibit   resonance;   this   assertion   will   be   clarified   later.   This

416 misinterpretation probably appears because of the fact that in the presence of
417 damping, the amplitudes jump from a large displacement equilibrium path to a
418 small displacement one, thus producing a resonance like response. Not only is
419 the jump frequency sensitive to damping, but also to the load amplitude. In
420 virtue of that, it is very important to note that, unlike linear oscillators, the
421 frequency tuning of a LBVEH is strongly dependent on the load amplitude and
422 on the system damping.
423   A reasonable criterion to maximize the velocity of the stack of magnets
424 relative to the coil is to maximize the stack stroke; which has the natural
425 consequence of increasing size. If sinusoidal excitation is assumed, the
426 harvester vibration frequency fixed, so maximizing the amplitude is the next
427 step. At this point, the geometric dimensions of the device define the elasticity
428 of the system. The harvester mass is fixed by the magnetic induction design
429 through the harvester power requirements.

430 ## 3. EQUATIONS OF MOTION

431 ### 3.1. Mechanical system

432   The equation of motion are derived from the force balance in the stack; we
433 will refer the displacements of the stack to the displacements of the cylinder;
434 therefore, the resulting formulation can be considered to be *relative*. Note that
435 an absolute formulation could also be derived, but it is clearly not advantageous
436 in cases where base acceleration is used as excitation since the evaluation of
437 the external forces is considerably more involved. In turn, if the base
438 displacement is chosen as excitation, an absolute formulation is advised.
439   Recalling Eqs. (4) and (5), the equations of motion can be written as

$$F_k(x, \varphi_m) + F_c(\dot{x}, \varphi_m') + F_g = m\ddot{x}_s, \tag{16}$$

440 being F_k, F_c and F_g the levitation, damping and gravitational forces respectively
441 and $\ddot{x}_s$ the absolute acceleration of the stack.
442   Using Eqs. (6), (9), (12) and (15) the equations of motion can be expanded as

$$m\ddot{x}_s + a_0^k u_s + a_3^k u_s^3 + a_5^k u_s^5 + \left[c_s + \frac{c_f}{|\dot{u}_s|} + \frac{(\sum \varphi_i')^2}{R_T}\right]\dot{u}_s \\ + mg = 0 \tag{17}$$

443   The stack acceleration can be obtained by derivation of Eq. (7), so

$$\ddot{x}_s = \ddot{u}_s + \ddot{x}_b \tag{18}$$

444   Defining the nonlinear stiffness

$$k(u_s) = a_0^k + a_3^k u_s^2 + a_5^k u_s^4 \tag{19}$$

445 And the damping coefficient

$$c = c_s + \frac{c_f}{|\dot{u}_s|} + \frac{(\sum \varphi_i')^2}{R_T} \tag{20}$$

446   The equations of motion can be written in the compact form

$$m\ddot{u}_s + k(u_s)u_s + c(\dot{u}_s, \varphi_i')\dot{u}_s = -m(\ddot{x}_b + g) \tag{21}$$

447   From the last equation, it can be clearly seen that all unknowns are relative
448   magnitudes.

3.2. Electrical system

450   As already said, the change in magnetic flux induces a voltage in the coils.
451   When the circuit is closed with a load, a current flows through the circuit. The
452   equations of the electrical system can be written as

$$L\dot{I} + R_T I = V \tag{22}$$

453   where I is the current flowing through the circuit, L is the inductance of the
454   coils, R_T is the total resistance of the circuit and V the induced voltage.
455   Using Eq. (3), the voltage can be expressed as a function of the stack velocity,
456   then the electrical system equations take the form

$$L\dot{I} + R_T I = -\sum \varphi_i' \dot{u}_s \tag{23}$$

457   As it can be seen, this is an electro-mechanical equation, coupled through
458   the derivative of the magnetic flux.

3.3. Coupled system

460   The electro-mechanical system is modeled by a coupled system of nonlinear
461   equations. Bringing together the mechanical and the electrical equations, Eq.
462   (21) and Eq. (23) respectively, we have

$$m\ddot{u}_s + k(u_s)u_s + c(\dot{u}_s, \varphi_i')\dot{u}_s = -m(\ddot{x}_b + g)$$
$$L\dot{I} + R_T I = -\varphi_i'\dot{u}_s \tag{24}$$

463   In matrix form the above equations can be written as

$$\begin{bmatrix} m & 0 \\ 0 & 0 \end{bmatrix}\begin{bmatrix} \ddot{u}_s \\ \dot{I} \end{bmatrix} + \begin{bmatrix} c_s + \dfrac{c_f}{|\dot{u}_s|} + \dfrac{\varphi_i'^2}{R_T} & 0 \\ \varphi_i' & L \end{bmatrix}\begin{bmatrix} \dot{u}_s \\ I \end{bmatrix} + \begin{bmatrix} k(u_s) & 0 \\ 0 & R \end{bmatrix}\begin{bmatrix} u_s \\ I \end{bmatrix} = \begin{bmatrix} -m(\ddot{x}_b + g) \\ 0 \end{bmatrix} \tag{25}$$

464   In order to numerically integrate this equations using the Runge-Kutta
465   algorithm the system must be recast in state space form, then

$$\begin{bmatrix} \dot{u}_s \\ \ddot{u}_s \\ \dot{I} \end{bmatrix} = \begin{bmatrix} 0 & 1 & 0 \\ -\dfrac{k(u_s)}{m} & -\dfrac{1}{m}c(\dot{u}_s, \varphi_i') & 0 \\ 0 & -\dfrac{\varphi_i'}{L} & -\dfrac{R_T}{L} \end{bmatrix}\begin{bmatrix} u_s \\ \dot{u}_s \\ I \end{bmatrix} + \begin{bmatrix} 0 \\ \ddot{x}_b + g \\ 0 \end{bmatrix} \tag{26}$$

466   Now, the last form of the system of equations is ready to be implemented in the
467   computational code.
468   It is important to note that the RK method is particularly attractive for
469   solving this class of problems since it can handle nonlinearities without
470   requiring the linearization of the equations of motion. This advantage is in some
471   way paid with the additional degree of freedom required to put the second order
472   equations of motion in the equivalent first order state space form.

3.4. Algorithmic structure

474   The equations of motion are implemented in a computational code called
475   PyDy. The code exploits the hybrid approach to evaluate the electromechanical
476   variables at each time step; the algorithmic structures is as follows:

477   • Read the harvester geometric and mechanical data.
478   • Read process the magnetic flux file according to the algorithm in
479   section 2.4.
480   • Initialize all variables.
481   • Do a time loop
482   ○ Do a coil loop
483   ▪ Calculate the flux derivative at the current coil via
484   interpolation of the flux file.
485   ▪ Add the result to the total flux derivative.
486   ○ Calculate the magnetic damping.
487   ○ Calculate the magnetic force at the current stack position using
488   the analytical force law.
489   ○ Form the state matrix and state vector.
490   ○ Solve for the state variables.

4. RESULTS AND VALIDATION

492   In order to validate the proposed approach a physical prototype of a LBVEH
493   was built. The key idea of the physical design is not to optimize the power
494   generation but to obtain a dynamical behavior such that the voltage signal is
495   composed by multiple magnet fluxes crossing different coils simultaneously;
496   this choice is made to test the framework in the most complex scenario. The
497   Table 1 shows the harvester parameters.
498   The harvester was designed with a multi-pole-multi-coil configuration that
499   generates a complex magnetic field distribution; thus, during operation the flux
500   gradient curve crosses different coils and a complex voltage signal is generated.
501   The coils were wounded with commercial wire of AWG30 gauge and connected
502   in series.
503   The stack was built by piling four neodymium magnets in repelling poles
504   configurations; steel spacers were added between the magnets in order to retain
505   the magnetic flux. The stack displacement is limited by the repelling force of two
506   end magnets, which are identical to those that form the stack; this choice allows
507   to generate a large displacement dynamics.
508

Symbol	Property	Value
h	Harvester stroke	100 mm
l	Harvester length	120 mm
d_h	Harvester diameter	28.0 mm
d_{co}	Cylinder outer diameter	20.5 mm
d_{ci}	Cylinder inner diameter	16.0 mm
n_m	Number of stack magnets	5
m_s	Stack Mass	48 gr.
d_m	Magnet diameter	15.0 mm
t_m	Magnet thickness	5.0 mm
t_s	Spacer thickness	5.0 mm
-	Magnet grade	N37
n_c	Number of coils	3
n_{cl}	Total number of coil loops	1850
d_w	Wire diameter (gauge)	0.24 mm (AWG30)

509   *Table 1- Harvester properties.*

4.1. Experimental setup

The physical prototype was excited with a electromechanical shaker a different frequencies and the voltage and base acceleration signals were acquired. The equipment used to conduct the tests was: Labworks ET-132 electrodynamic shaker, Rigol DG 4062 function generator, home-built amplifier, PCB Accelerometer and National NI9234 data acquisition module.

The harvester was excited at different discrete frequencies between 2 and 10 Hz. The piezoelectric accelerometer was mounted in the base of the shaker in order to use this signal as an excitation for the computational model.

The formulation was implemented in a Python code written by the authors called PyDy, which is based on the Object Oriented Programming philosophy and a Runge-Kutta Method solver.
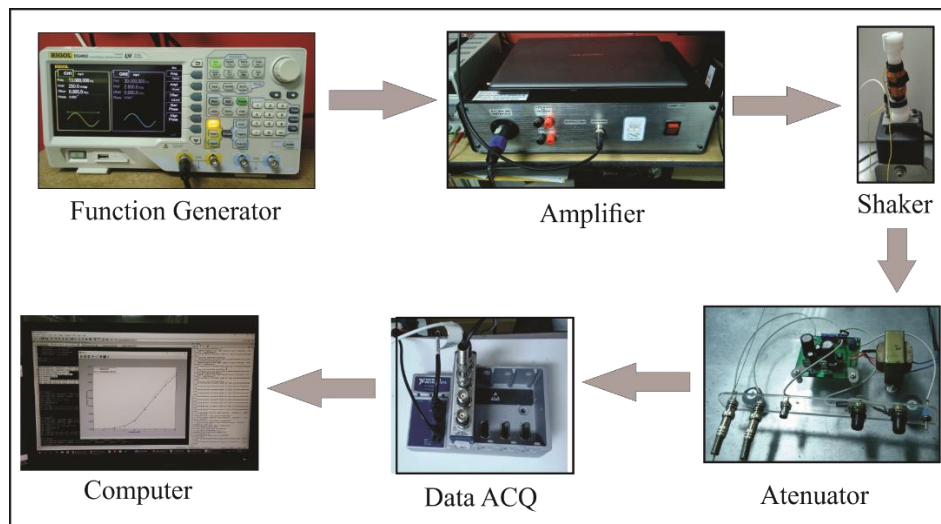

Figure 7 – Data acquisition hardware configuration

4.2. Damping identification

The present approach includes the effects of both viscous and friction damping. The friction damping is expected to influence the system dynamics in the low frequency range; viscous damping is expected to do it in the high frequency range.

Both damping effects are modeled through proportional models with frequency varying coefficients, which are a function of velocity and its determination require an "identification" procedure. Especially the friction coefficient is very difficult to identify since the normal force is intermittent. This intermittence is very difficult to eliminate without closing the gap between the stack and the cylinder, which has the drawback of increasing the effective friction force and consequently the value of damping. In order to simplify the identification of the damping coefficients, we have assumed that the stack moves at the same frequency of the signal and then identified discrete values of damping for certain frequencies.

The Figure 8 shows the simulated and measured voltage signals at an operation frequency of 2 Hz for different friction coefficients, the viscous damping coefficient was set to 0.25.
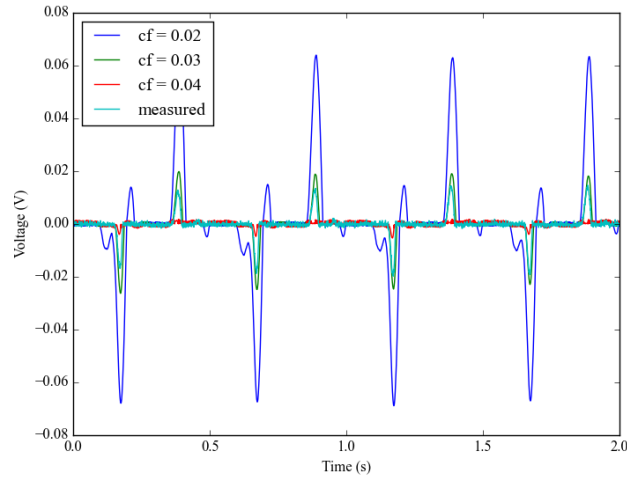
542

543 *Figure 8 – Effect of the frictional force*

544   It can clearly be seen that friction governs the intermittence of the stack
545 motion; the stack moves only when the inertial force is larger than the frictional
546 force.
547   The Figure 9 shows the correlation between the experiment and the
548 simulation for one period of motion setting the frictional damping coefficient at
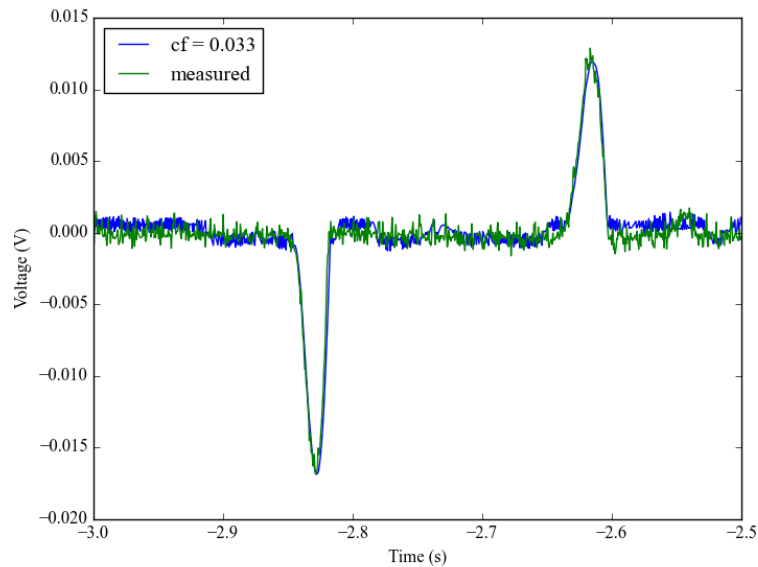549 0.33.

550

551 *Figure 9 – Friction coefficient identification – 2.0 Hz*

552   As the excitation frequency increases the effect of the friction damping is less
553 important and the viscous damping terms governs the damping forces. The
554 Figure 10 shows the correlation of the voltage signal between the experiment
555 and the simulation for a base excitation of 10.0 Hz. The optimal viscous damping
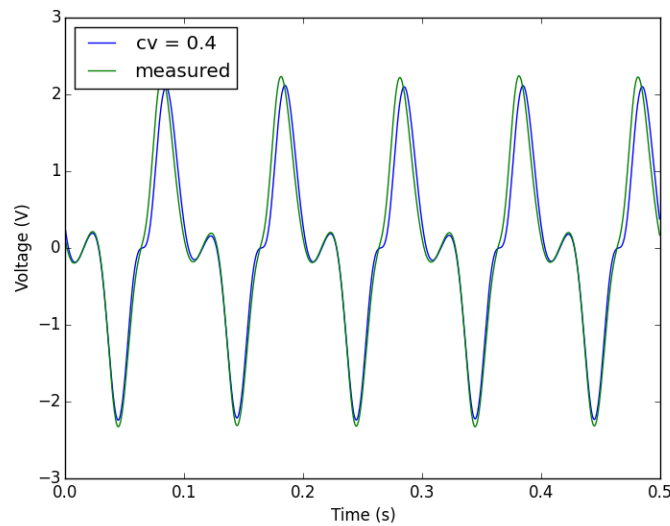556 coefficient is 0.4.

Note that obtaining such a good correlation of the voltage signal in the time domain is actually difficult since it is dictated by the product of two functions that are changing in space and time, the velocity and the magnetic flux derivative.

4.3. On the existence of resonance

Most investigations about magnetic levitation based energy harvesters (LBVEH) assume that the harvester must work at resonance to scavenge the maximum energy [6,7,8,11]. However, the harvester behaves as a Duffing oscillator, which do no exhibit resonance [24]. Resonance is defined as a property of the system and thus it must be independent of the external forces. But this is not the case of an oscillator with nonlinear stiffness, since the stiffness is a function of the displacement; then it could be said the system has a "continuously varying natural frequency". Note that the displacement amplitude of an undamped LBVEH increases continuously with frequency, and the maximum amplitude is found when the forcing frequency is infinity.

When the system is damped, the stack amplitude does not increase continuously with the frequency of the excitation; for a certain frequency, the response falls suddenly from a large displacement equilibrium to a small displacement equilibrium. The phenomenon is called "jump" and is typical of the Duffing oscillator. The frequency location of the maximum amplitude is not only a function of the system, but also of the load amplitude and the system damping.

4.4. Generated power

The ultimate objective of the proposed computational procedures is to obtain an accurate estimation of the harvested energy. The electrical power is a function of the induced voltage and the current flowing in the circuit; both variables are related through the circuit load. In order to simulate the power consumption of a small electronic device we have represented the load with a resistance of 100 Ohm.

589   The Figure 11, Figure 12 and Figure 13 show the correlation of the peak
590   voltage for an input acceleration of 1g, the average power and the peak power
591   between the present computational approach and the physical experiment. The
592   tests were performed at discrete values of excitation frequencies in order to avoid
593   transient effects; the base accelerations measured in the physical tests were
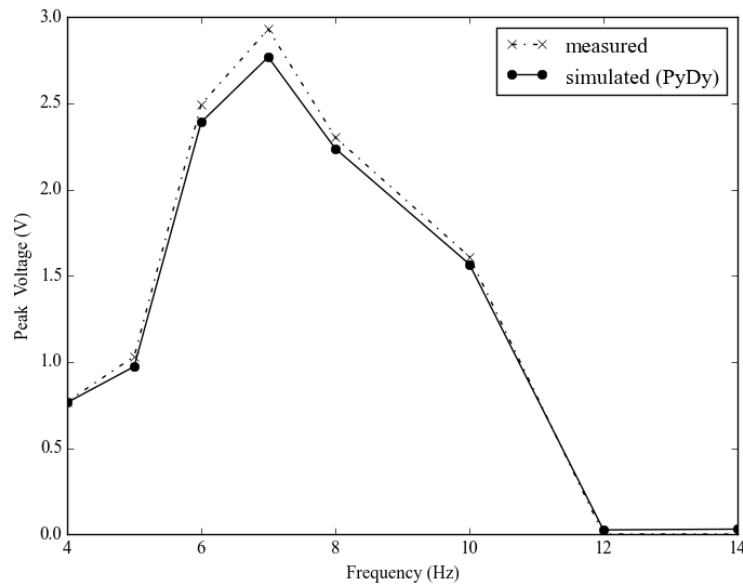594   used as input of the simulation.

Figure 11 – Peak Voltage (1g)

595
596

597   The peak voltage values given by the present approach correlate very well
598   with the experiment, see Figure 11. It must be noted that in order to obtain
599   accurate values of the peak voltage it must be ensure that the excitation of the
600   computational model is the same than the excitation of the experiment;
601   especially if the shaker dimensions are such that the system inertial forces
602   affects its dynamics.
603   Regarding the power values, both the peak and the average power show a
604   good agreement between the experiment and the simulation. It is important to
605   mention that the time signals of power are directly obtained from the voltage
606   signal, which also shows an excellent correlation between the simulation and
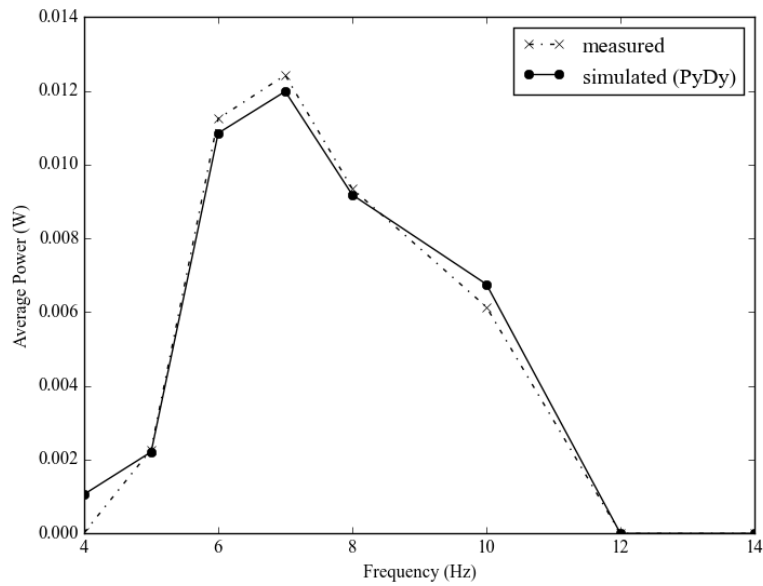607   the experiment; see Figure 8, Figure *9* and Figure *10*.
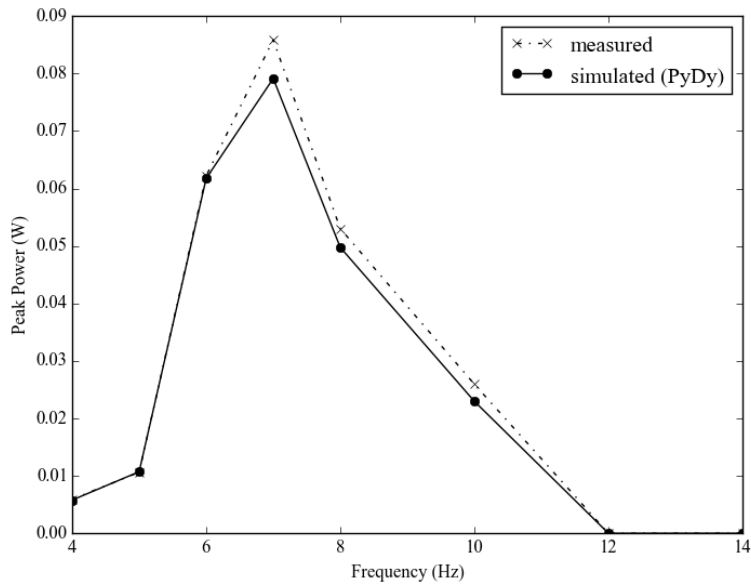
Figure 12 – Average Power (1g)

Figure 13 – Peak Power (1g)

5. CONCLUSIONS

A hybrid numerical-analytical approach for the design of levitation based vibration energy harvesters has been presented. The coupled equations of motion of the 2 DOF electromagnetic system were written in terms of an analytical function for the levitation force and a numerically interpolated function for the magnetic flux derivative. The approach can model harvesters with arbitrary magnet-coil-spacer configurations; it allows arbitrary excitations and arbitrary nonlinearities.

The levitation force function was obtained via polynomial fitting of discrete force measurements of a finite element model. It was shown that numerical modeling of the levitation force and the magnetic flux can be embedded into the electromagnetic dynamic equations to permit modeling of any multi-pole-multi-coil configuration. Using the same finite element model a numerical function of the average magnetic flux density as a function of the spatial coordinate was extracted. This function was derivate numerically and then smoothed through a Savitzky-Golay filter.

The dynamic response of a multi-magnet-multi-coil harvester was analyzed; it was shown that the maximum displacement frequency is strongly dependent on damping and on the excitation amplitude. It was also shown that the response of the harvesters does not exhibit a behavior analogous to the linear oscillator resonance.

A performance assessment by comparing the results obtained with the present formulation against measurements was presented; a physical prototype of a multi-pole-multi-coil harvester is built ad hoc. It was shown that the approach gives excellent results in terms of: prediction of the voltage-time signal and estimation of integrated parameters as average power and average voltage.

REFERENCES

[1] A. Abdelkefi, Aeroelastic energy harvesting: A review, Int. J. Eng. Sci. 100 (2016) 112–135. doi:10.1016/j.ijengsci.2015.10.006.

[2] A.R.M. Siddique, S. Mahmud, B. Van Heyst, A comprehensive review on vibration based micro power generators using electromagnetic and piezoelectric transducer mechanisms, Energy Convers. Manag. 106 (2015) 728–747. doi:10.1016/j.enconman.2015.09.071.

[3] M.Q. Le, J.-F. Capsal, M. Lallart, Y. Hebrard, A. Van Der Ham, N. Reffe, L. Geynet, P.-J. Cottinet, Review on energy harvesting for structural health monitoring in aeronautical applications, Prog. Aerosp. Sci. 79 (2015) 1–11. doi:10.1016/j.paerosci.2015.10.001.

[4] H.S. Kim, J.H. Kim, J. Kim, A review of piezoelectric energy harvesting based on vibration, Int. J. Precis. Eng. Manuf. 12 (2011) 1129–1141. doi:10.1007/s12541-011-0151-3.

[5] A. Harb, Energy harvesting: State-of-the-art, Renew. Energy. 36 (2011) 2641–2654. doi:10.1016/j.renene.2010.06.014.

[6] H. Xiao, X. Wang, A review of piezoelectric vibration energy harvesting techniques, Int. Rev. Mech. Eng. 8 (2014) 609–620. doi:10.4028/www.scientific.net/AMM.44-47.2945.

[7] G. De Pasquale, S. Iamoni, A. Somà, 3D numerical modeling and experimental validation of diamagnetic levitating suspension in the static field, Int. J. Mech. Sci. 68 (2013) 56–66. doi:10.1016/j.ijmecsci.2012.12.018.

[8] M.P. Soares Dos Santos, J.A.F. Ferreira, J.A.O. Simões, R. Pascoal, J. Torrão, X. Xue, E.P. Furlani, Magnetic levitation-based electromagnetic energy harvesting: a semi-analytical non-linear model for energy

672   transduction., Sci. Rep. 6 (2016) 18579. doi:10.1038/srep18579.

673 [9]   D.J. Apo, S. Priya, High Power Density Levitation-Induced Vibration
674   Energy Harvester, Energy Harvest. Syst. 1 (2014) 79–88.
675   doi:10.1515/ehs-2013-0005.

676 [10]   B.P. Mann, N.D. Sims, Energy harvesting from the nonlinear oscillations
677   of magnetic levitation, J. Sound Vib. 319 (2009) 515–530.
678   doi:10.1016/j.jsv.2008.06.011.

679 [11]   Y. Zhu, J.W. Zu, A magnetoelectric generator for energy harvesting from
680   the vibration of magnetic levitation, IEEE Trans. Magn. 48 (2012) 3344–
681   3347.

682 [12]   S. Palagummi, J. Zou, F.G. Yuan, A Horizontal Diamagnetic Levitation
683   Based Low Frequency Vibration Energy Harvester, J. Vib. Acoust. 137
684   (2015) 61004. http://dx.doi.org/10.1115/1.4030665.

685 [13]   I. Abed, N. Kacem, M.L. Bouazizi, N. Bouhaddi, Shock & Vibration,
686   Aircraft/Aerospace, and Energy Harvesting, in: Proc. 33rd IMAC, A Conf.
687   Expo. Struct. Dyn., 2015: p. Chapter 5.

688 [14]   C. Lee, D. Stamp, N.R. Kapania, J.O. Mur-Miranda, Harvesting vibration
689   energy using nonlinear oscillations of an electromagnetic inductor,
690   Energy. 7683 (2010) 76830Y–76830Y–12. doi:10.1117/12.849895.

691 [15]   A. Munaz, B.C. Lee, G.S. Chung, A study of an electromagnetic energy
692   harvester using multi-pole magnet, Sensors Actuators, A Phys. 201 (2013)
693   134–140. doi:10.1016/j.sna.2013.07.003.

694 [16]   E. Dallago, M. Marchesi, G. Venchi, Analytical model of a vibrating
695   electromagnetic harvester considering nonlinear effects, IEEE Trans.
696   Power Electron. 25 (2010) 1989–1997. doi:10.1109/TPEL.2010.2044893.

697 [17]   A.G. Avila Bernal, L.E. Linares García, The modelling of an
698   electromagnetic energy harvesting architecture, Appl. Math. Model. 36
699   (2012) 4728–4741. doi:10.1016/j.apm.2011.12.007.

700 [18]   X.Y. Wang, S. Palagummi, L. Liu, F.G. Yuan, A magnetically levitated
701   vibration energy harvester, Smart Mater. Struct. 22 (2013) 55016.
702   doi:10.1088/0964-1726/22/5/055016.

703 [19]   G. De Pasquale, A. Somà, F. Fraccarollo, Comparison between
704   piezoelectric and magnetic strategies for wearable energy harvesting, J.
705   Phys. Conf. Ser. 476 (2013) 12097. doi:10.1088/1742-
706   6596/476/1/012097.

707 [20]   C.R. Saha, T. O'Donnell, N. Wang, P. McCloskey, Electromagnetic
708   generator for harvesting energy from human motion, Sensors Actuators,
709   A Phys. 147 (2008) 248–253. doi:10.1016/j.sna.2008.03.008.

710 [21]   D.J. Griffiths, C. Inglefield, Introduction to Electrodynamics, 2005.
711   doi:10.1119/1.4766311.

712 [22]   D.J. Griffiths, Introduction to electrodynamics,Griffith-3ed.pdf, 2010.
713   doi:10.1119/1.4766311.

714 [23]   D.C. Meeker, Finite Element Method Magnetics, Version 4.0.1
715   (03Dec2006 Build), (n.d.) http://www.femm.info.

716 [24]   L. Meirovitch, Elements of Vibration Analysis, (1986) 560.
717   doi:10.1016/S0022-460X(87)80083-4.

718